DOI: 10.1002/ejic.201001355

The U_{28} Nanosphere: What's Inside?

May Nyman,*[a] Mark A. Rodriguez,[a] and Todd M. Alam[a]

Keywords: Cluster compounds / Peroxides / Polyanions / Polyoxometalates / Uranium

Polyoxometalate-like behavior of actinyl-peroxide anions in aqueous alkaline media has been recently unveiled in the form of more than 20 reported crystal structures of clusters, each with 20–60 uranyl polyhedra composing capsule-like topologies. There is now opportunity to fully develop this new polyoxometalate (POM) family to include redox behavior, non-aqueous chemistry, complex materials from cluster building blocks, cluster-counterion interactions, etc. To pursue these opportunities, reliable syntheses rooted in an understanding of cluster assembly processes are imperative. To this end, using the U_{28} nanosphere $[UO_2(O_2)_{1.5}]_{28}$ as an example, we report high yield syntheses of a series of four U_{28} salts that feature different templating cations (K, Rb, Cs) and anions [uranyl monomer, $Nb(O_2)_4$ and $Ta(O_2)_4$]. The key to assembly and stability of U_{28} is both 1) synthetic conditions that are not extreme or dynamic, and 2) templating cations and anions that ideally match each other and the topology of the capsule interior. U_{28} salts are characterized in the solid-state by powder and single-crystal X-ray diffraction and infrared spectroscopy. Furthermore, Cs-templated U_{28} is re-dissolved and characterized by ^{133}Cs NMR; providing information on solution stability, and revealing the interaction of the internal templating Cs^+ with the central templating anion. While Cs^+ internal to the cluster remains inside when U_{28} is dissolved in a Na salt solution, the internal K^+ will rapidly exchange with Na^+, providing new routes to other cluster topologies and compositions.

Introduction

The chemistry of uranyl(VI) peroxide ions is rich and fascinating. Uranyl peroxide phases form in the aqueous environment and in anthropogenic settings such as nuclear fuel storage pools; despite the only source of the peroxide ligand is from α-hydrolysis of water.[1] This apparent stability of the uranyl-peroxide bond suggests its importance in aqueous chemistry, facilitating oxidation, dissolution, complexation, transport and precipitation in nature and in nuclear waste and fuel storage containments. Furthermore, trans-Uranics, especially neptunyl exhibits similar behavior.[2] Thus the peroxide ligand must be considered in developing nuclear fuel reprocessing and radionclide separation chemistries, as well as models for actinide transport in the bio-geosphere.

Recognizing this ubiquity of the actinyl-peroxide bond, Burns and co-workers[2e] in 2005 unveiled an entirely new class of actinide clusters featuring edge-sharing $UO_2(O_2)_3$ polyhedra assembled into spherical multinuclear anions containing up to 60 uranium atoms.[3] These were all crystallized from very concentrated solutions containing >3 molar alkali hydroxide, >20% peroxide and >0.1 molar uranyl nitrate. Solutions such as these containing high hydroxide and peroxide concentrations, and that are located in uncontrolled ambient conditions are dynamic with continuous O_2 evolution, carbonate adsorption and resulting pH change. Given the inconsistent and dynamic nature of these mother liquors from which uranyl peroxide nanospheres are obtained, it is not surprising that extremely low yields or mixed phases have been reported. In the most extreme case, a lone crystal of $[UO_2(O_2)_{1.5}]_{28}$ (U_{28}) was reported as a yield.[2e] Yet, in order to fully realize the chemistry of uranyl peroxide nanospheres, we need reproducible syntheses, sufficiently high yields and stable materials for in-depth solution and solid-state studies.

Using U_{28} as an example we have fully developed synthetic procedures that provide high yields of pure materials, reproducibly. Our methods are based on 1) utilizing synthesis conditions that are not extreme nor rapidly evolving; 2) stragic use of cations and anions that appear to play a key role in internally templating the spherical shell of edge-sharing uranyl peroxide anions; and 3) ion exchange of counterions-inside and outside the U_{28} capsule. Furthermore, the choice of templating cations and anions appear to affect the solution behavior and stability of these clusters.

Results and Discussion

U_{28} consists of four hexagonal rings [six edge-sharing $UO_2(O_2)_3$ polyhedra] and twelve pentagonal rings [five edge-sharing $UO_2(O_2)_3$ polyhedra]. The hexagonal rings are organized in a tetrahedral arrangement and each of the twenty-eight uranyl polyhedra is at the junction of either

[a] Sandia National Laboratories,
Albuquerque, NM 87185, USA
Fax: +1-505-844-7354
E-mail: mdnyman@sandia.gov

Supporting information for this article is available on the WWW under http://dx.doi.org/10.1002/ejic.201001355.

Table 1. Bond data for templating alkali (K^+, Rb^+, Cs^+) for U_{28} analogues.

	Hexagonal ring A–O / Å (A = K, Rb, Cs)	BVS	O_{yl}–A–O_{yl} angles / ° [b]	Pentagonal ring K–O / Å	BVS
$CsKU_{28}$ (1)					
A–O_{yl} bonds[a]	3.20	**0.76**	159–163	2.75	1.00
$RbKU_{28}$ (2)					
A–O_{yl} bonds[a]	3.12	**0.57**	157–176	2.72	1.08
Bond to external water[c]	2.88	0.091			
Including all bonds		**0.661**			
KKU_{28} (3)					
A–O_{yl} bonds[a]	3.08	**0.49**	170–177	2.68	1.205
Bond to external water[d]	2.67	0.124			
Including all bonds		**0.614**			
Nb-$RbKU_{28}$ (4)					
A–O_{yl} bonds[a]	3.07	**0.654**	182	2.70	1.15
Bond to external water[e]	2.95	0.152			
Two bonds to $Nb(O_2)_4$	3.356	0.100			
Including all bonds	3.081	**0.906**			
Ta-$CsKU_{28}$ (5)					
A–O_{yl} bonds[1]	3.16	**0.84**	167–198	2.72	1.08
Bond to external water[f]	3.20	0.063			
Including all bonds[g]		**0.903**			

[a] Average A–O (A = K, Rb, Cs) bond lengths within the pentagonal or hexagonal rings of U_{28}. [b] O_{yl}–A–O_{yl} bonds greater than 180° are bent so that the Rb/Cs points towards the center of the sphere. O_{yl}–A–O_{yl} bonds less than 180° are bent so that the Rb/Cs points toward the outside of the sphere. [c] Half the internal Rb (Rb2 and Rb3) have bonds to external water. [d] Half the hexagonally-bound internal K is bonded to external water. [e] Each internal Rb (Rb1) is bonded to external water. [f] Half the internal Cs (Cs1 and Cs2) have bonds to external water. [g] This evaluation for **5** does not include the bonds to the central $Ta(O_2)_4$ because not all the peroxo oxygen atoms were located.

three pentagonal rings or two pentagonal rings plus one hexagonal ring (Figure 1, a and b). The structure originally reported in 2005[2e] was a mixed Li^+/K^+ salt where inside the U_{28} sphere, a K^+ cation templates every pentagonal and hexagonal ring, with a formula (including the internal cations only) of $[K_{16}\{(UO_2)(O_2)_{1.5}\}_{28}]$. Both the pentagonal and hexagonal rings serve as perfect inorganic crowns for cations: the internal "*yl*" oxygen atoms that bond the alkali point inward towards the center of the ring, as the ring is a curved portion of the uranyl peroxide capsule. While the pentagonal ring is an ideal size for K^+, the hexagonal ring is a little large based on bond valence sum (BVS)[4] theory (see Table 1; discussed below). The larger hexagonal ring is more suitable to host Rb or Cs cation, and this is also the result obtained from recent computational studies.[5]

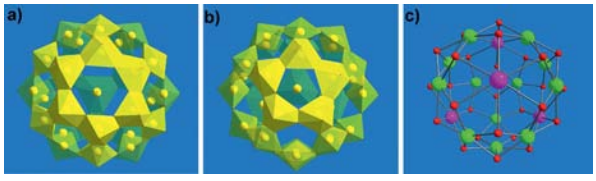

Figure 1. Three views of the U_{28} capsule, $[A_{16}(UO_2)_{28}(O_2)_{42}]$ (A = alkali; K, Rb, Cs). View of the uranyl polyhedra (yellow) through a hexagonal ring (a) and pentagonal ring (b). Alkali's are omitted for clarity. (c) View of the alkalis that reside inside the U28 capsule (green in the twelve pentagonal rings; pink in the four hexagonal rings) bonded to the internal *yl* oxygens (red) of the uranyl polyhedra.

Synthesis

Our first synthetic strategy is to utilize aqueous media containing both larger (Rb, Cs) and smaller (K) templating cations. Furthermore, we have developed synthesis techniques that provide less harsh and dynamic conditions than those reported prior. For example, a cooled solution of uranyl nitrate (5 °C) is added to a cooled solution of peroxide/hydroxide containing KOH plus RbCl or CsCl to give a 4:1 ratio of K:Rb/Cs. Under these conditions, there is rapid and spontaneous precipitation of a bright yellow K-Rb/Cs $UO_2(O_2)_3$ salt that has an approximate formula of $A_4UO_2(O_2)_3{\cdot}10H_2O$ (A = K, Rb/Cs) and the alkali ratio of the precipitate reflects that of the precursor solution. If the solution is warmed to room temperature, the precipitate rapidly redissolves. Furthermore, once isolated in the solid form, the stability of this salt is limited, as indicated by its reddening in color and loss in aqueous solubility. Thus, the precipitate is immediately and rapidly isolated by vacuum filtration and dried by washing with alcohol. This precipitate then readily dissolves in DI water, from which the U_{28} salt precipitates. Thus, excessive hydroxide and peroxide is eliminated from the synthesis media, so rapid decomposition of peroxide and the accompanying O_2 bubble formation is minimized. Furthermore, the synthesis pH is consistently ca. 11.5, as apposed to >13. Crystallization time varies from almost immediately to several days, depending on the templating ions and countercations: for instance the Cs salts precipitate much more rapidly than the Rb analogues. Although all syntheses reported here are based on 1 mmol uranyl nitrate, we have also shown that the reaction is readily scaled up, producing multi-gram yields. Single-crystals for X-ray analyses in every case are representative of the bulk precipitate, see Figure 2, for example (also see Supporting Information). This also provides evidence for the pure and abundant nature of these U_{28} salts.

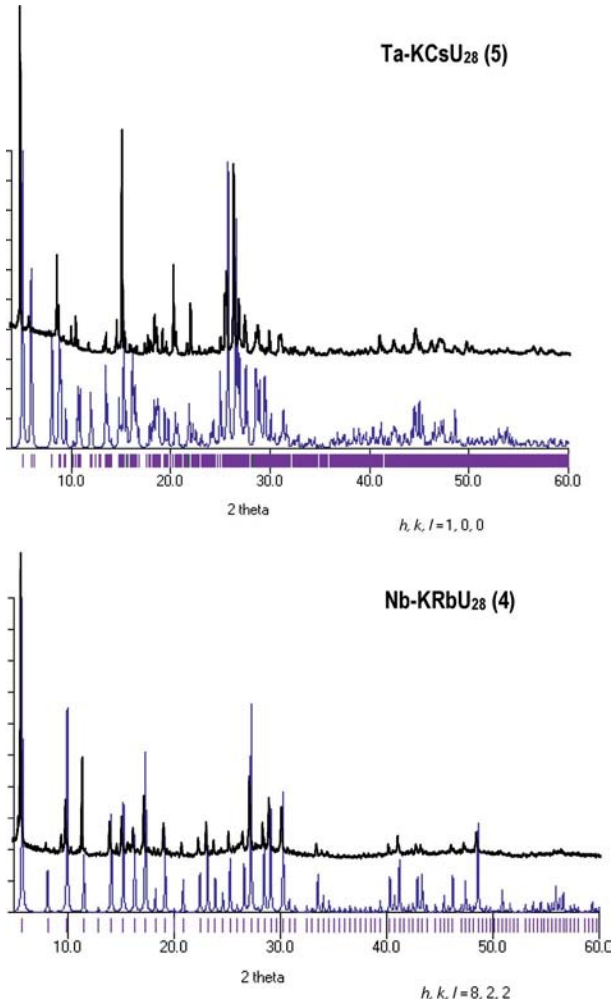

Figure 2. Powder diffraction spectra (black), calculated spectra from single-crystal data (blue) and peak positions (purple) for **Ta-KCsU$_{28}$** (**5**) and **Nb-KRbU$_{28}$** (**4**).

Effect of Internal Templating Cation

Isostructural $Cs_{16}[Cs_4K_{12}[(UO_2)(O_2)_3]\{(UO_2)(O_2)_{1.5}\}_{28}]\cdot 11H_2O$ (**1**) and $Rb_{12.5}K_{3.5}[Rb_4K_{12}[(UO_2)(O_2)_3]\{(UO_2)(O_2)_{1.5}\}_{28}]\cdot 18.5H_2O$ (**2**) (Table 2) were characterized by single-crystal X-ray diffraction; and indeed the four hexagonal rings host the Rb and Cs cations, respectively while the twelve pentagonal ring host the K^+ cations (Figure 1**c**). In Table 1, we compare the A–O_{yl} (A = K,Rb,Cs) bond lengths of the alkalis templating the inside of the U_{28} cluster of **1**, **2** and **3**; where **3** is $[K_{16}\{(UO_2)(O_2)_{1.5}\}_{28}]$ originally reported by Burns in which K^+ is located inside every pentagonal and hexagonal ring of the cluster.[2e] Compounds **1**, **2** and **3** are denoted $CsKU_{28}$, $RbKU_{28}$ and KKU_{28}, respectively. In Table 1, we use A^+ BVS, considering only the oxygens from the uranyl ring, as a figure of merit for size-matching of the ring to the alkali. Based on this parameter, the pentagonal ring is nearly ideal for K^+. The BVS. for K, Rb, and Cs are all low in the hexagonal ring, with the "fit" improving from K to Rb to Cs. However, in this evaluation, we do not consider the oxygens of the central anion nor any water bound from the outside of the sphere.[6] Regarding the oxygen atoms bonded to the uranyl complex that fully occupies the center of **1** and **2** and has a 0.4 occupancy at the center of **3**; these are poorly defined, an averaging of an orientationally-disordered anion. For charge-balance requirements, as well as considering commonly observed species under these conditions, we assumed the central uranyl complex in **1** and **2** to be $UO_2(O_2)_3^{4-}$, but we could not reasonably fix any oxygen-ligand positions. In **3**, oxygen positions were assigned to a complex described as ~4/10th $UO_2(H_2O)_2(O_2)_2^{3-}$, again to suit charge-balancing requirements, but the ligand geometries are not ideal. In other words, it is not possible to determine how this disordered anion binds the internal alkali shell of U_{28}, but it

Table 2. Crystallographic information for $Cs_{16}[Cs_4K_{12}[(UO_2)(O_2)_3]\{(UO_2)(O_2)_{1.5}\}_{28}]\cdot 11H_2O$ ($KCsU_{28}$, **1**), $Rb_{12.5}K_{3.5}[Rb_4K_{12}[(UO_2)(O_2)_3]\{(UO_2)(O_2)_{1.5}\}_{28}]\cdot 18.5H_2O$ ($KRbU_{28}$, **2**), $K_{12}Rb_3[Rb_4K_{12}[Nb(O_2)_4]\{(UO_2)(O_2)_{1.5}\}_{28}]\cdot 52H_2O$ (Nb-$KRbU_{28}$, **4**), and $Cs_{15}[(Ta(O_2)_4)\text{-}Cs_4K_{12}(UO_2(O_2)_{1.5})_{28}]\cdot 11H_2O$ (Ta-$KCsU_{28}$, **5**).

	1	**2**	**4**	**5**
Empirical formula	$H_{22}Cs_{20}K_{12}O_{159}U_{29}$	$H_{37}K_{15.5}O_{166.5}Rb_{16.5}U_{29}$	$H_{104}K_{24}NbO_{200}Rb_7U_{28}$	$H_{22}Cs_{19}K_{12}O_{170}TaU_{28}$
Formula weight	12596	11618	11596	12582
Crystal system	monoclinic	monoclinic	cubic	monoclinic
Space group	$P2_1/m$ (#11)	$P2_1/m$ (#11)	I 2 3 (#197)	$P2_1/m$ (#11)
a [Å]	19.6811(76)	19.4427(68)	21.6666(31)	19.8262(28)
b [Å]	28.5814(112)	28.2059(97)		28.4844(42)
c [Å]	19.6967(77)	19.4501(68)		19.8239(29)
β [°]	118.41(1)	118.74(1)		118.91
Volume [Å^3]	9745(7)	9352(6)	10171(3)	9801(2)
Z	2	2	2	2
$d_{calcd.}$ [g/cm^3]	4.26	4.07	3.894	4.219
Min./max. θ [°]	1.18/25.35	1.19/25.59	1.33/25.36	1.17/25.00
Final R_1[a] [$I > 2\sigma(I)$]	0.0950	0.0971	0.0366	0.0713
Final wR_2[b] [$I > 2\sigma(I)$]	0.155	0.1478	0.0521	0.1139
GOF	1.102	1.100	1.125	1.119

[a] $R_1 = \Sigma||F_o| - |F_c||/|F_o|$. [b] $wR_2 = \{\Sigma[w(F_o^2 - F_c^2)^2]/\Sigma[w(F_o^2)^2]\}^{0.5}$.

undoubtedly bonds these alkalis, especially the larger Rb and Cs. Since the central uranium in **1** and **2** had considerably larger thermal parameters than the uranium-sites within the cluster (i.e., U11 is about 0.1 for the central uranium, and 0.02 for the cluster uraniums), we also considered partial occupancy at this site. However, this change resulted in slightly worse agreement indices, and did not provide identification of the oxygen ligands bound to the central uranium. It is however not unreasonable that this central isolated uranyl anion which is clearly disordered has higher mobility than the uranyl polyhedra within the rigid framework of the nanosphere. The pentagonal K^+ cations in **1** and **2** are best described as two half occupied positions; one forms almost a flat plane with its five bonds to the *yl*-oxygen atoms of the pentagonal ring (K_{outer}), and one inward towards the center of the sphere (K_{inner}). The distances between the two half-occupied positions range from 0.68–1.12 Å. This disorder indicates motion of K^+ cations templating the pentagonal rings. In contrast; in the structure of **3**, a single K-site that sits in the plane of the pentagonal *yl*-oxygen atoms was identified. However, the unit-cell of **3** is approximately twice as large as the cells of **1** and **2**, and for **3**, half the K^+ fully occupy the K_{inner} position and half the K^+ fully occupy the K_{outer} position.[7]

The increasing $A–O_{yl}$ bond length from K to Rb to Cs sited in the hexagonal ring is achieved by the alkali moving away from the center of the sphere. This can be viewed quantitatively in the $O_{yl}–A–O_{yl}$ bond angles; increasing in the order Cs < Rb < K. The range in these bond angles are also summarized in Table 1. The large range for **2** is because, like the pentagonally-coordinated K^+ cations, two of the four Rb^+ cations in **2** are in two half-occupied positions. This hexagonal ring is undoubtedly better sized for larger cations, given the increase of the BVS towards an ideal value of 1, from K to Rb to Cs. Even stronger evidence is the self-selection of this site by Rb and Cs during assembly and crystallization of **1** and **2** from mixed alkali (K/Rb and K/Cs) precursors. Finally, while one single crystal of **3** was reported to be obtained from a mixed Li/K precursor solution, we repeatedly obtain 60–75% yields of **1** and **2** respectively from Cs/K and Rb/K precursors, and the strong templating ability of Rb/Cs for the hexagonal ring likely plays a role in the process of U_{28} self-assembly.

Effect of Central Templating Anion

In interest of optimizing the U_{28} synthesis for yield, stability and reproducibility, we next turned our attention to the central anion. The uranyl anions such as $UO_2(O_2)_3^{4-}$ that partially-occupy the center of U_{28} in **3** and fully occupy the center in **1** and **2**, do not have a symmetry that matches that of the alkali and uranyl shells, and thus is probably not the ideal anion for templating this spherical cluster. The tetrahedral arrangement of the hexagonal rings and its templating alkali cations inspired us to consider other anions that feature tetrahedral geometry and are stable in highly alkaline and peroxide rich environments. The Group V peroxometalates [$Nb(O_2)_4^{3-}$, $Ta(O_2)_4^{3-}$] illustrated in part a of Figure 3 proved ideal. Whether this anion is introduced to the synthesis mixture as the hexametalate polyoxoanion $A_8[M_6O_{19}]{\cdot}xH_2O$[8] or the $A_3M(O_2)_4$[9,10] salt (M = Nb, Ta; A = K, Rb, Cs), the result is always the same: high yield of pure $M(O_2)_4$-centered U_{28}.

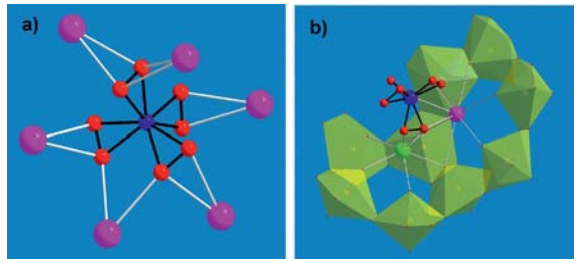

Figure 3. (a) Illustration of $A_3M(O_2)_4$ salt; A = K, Rb, Cs and M = Nb, Ta, showing the two modes of bonding of the peroxide ligands to the alkalis. (b). Internal view of a section of Nb-KRbU_{28} (**4**) illustrating the bonding of the central $Nb(O_2)_4$ anion to the templating K^+ and Rb^+ cations. For both (a) and (b), pink spheres are Rb, green sphere is K, red spheres are O, blue sphere is Nb, yellow octahedra are $UO_2(O_2)_3$.

Introduction of this templating anion provides opportunity to delineate the roles of the templating alkalis (Rb/Cs) vs. the synthetic procedure. In this experiment, we carried out the synthesis steps with K^+ as the only alkali and the addition of the peroxoniobate or peroxotantalate anion. These gave products that diffracted poorly, and infrared spectroscopy suggested it was a mixture of uranyl peroxide polyanions that did include some U_{28}. This provides more evidence that the larger hexagonal-templating alkali is important for the formation of U_{28}, and perhaps the Group V peroxoanion is synergistic in U_{28} templating via bonding between these two species. Nonetheless, it is self-evident that the tetrahedral $Nb(O_2)_4$ or $Ta(O_2)_4$ anion perfectly matches both the size and symmetry of the U_{28} cluster.

Obtaining the structure of $K_{12}Rb_3[Rb_4K_{12}[Nb(O_2)_4]\text{-}\{(UO_2)(O_2)_{1.5}\}_{28}]{\cdot}52H_2O$ (**4**), also referred to as Nb-KRbU_{28}, from a mixed K/Rb-$UO_2(O_2)_3$ precursor (see experimental for details) gave a clearer snapshot of the bonding between the central anion and ring-templating cations. While **1** and **2** were monoclinic, **4** crystallized in the *I*23 (#197) cubic space group. The different symmetry of **4** compared to the other structures reported here is likely related to the crystallization rate, rather than directed by the $Nb(O_2)_4$-central anion. This phase crystallized the slowest of this study for two reasons: 1) as described above, the mixed K-Rb salts are much more soluble in the mother liquors than the K-Cs salts, and 2) the Nb-source was the $[Nb_6O_{19}]^{8-}$ anion, so the $Nb(O_2)_4$ was apparently generated in-situ as the uranyl peroxide monomers released peroxide ligands during cluster assembly. We have also synthesized Ta-KRbU_{28} and Nb-KCsU_{28} (from $K_3Nb(O_2)_4$). These likewise exhibited the monoclinic symmetry, as determined by powder X-ray diffraction and cell-determination from single-crystals. Thus we can conclude that the $P2_1/m$ space group is in fact the most likely for these U_{28} salts to crys-

tallize in, and the cubic phase was obtained only in the special case of very slow crystal growth.

In **1** and **2**, the pentagonally-bound K^+ is modeled as two half-occupied positions. However, in **4**, the two K^+ sites are better modeled as 1/3rd occupied in the site closer to the center (K_{inner}), and 2/3rd occupied in the site towards the outside (K_{outer}) of the sphere. The central $Nb(O_2)_4$ is also disordered, and the disorder correlates with the disorder of templating K^+. Each peroxide ligand has three orientations, defined by a triangle of three 2/3rd -occupied oxygen-sites. Two of the three orientations of this ligand puts an oxygen too close to the K_{inner} (1.9 Å), which is why this site is 1/3rd occupied. Part b of Figure 3 illustrates the bonding of $Nb(O_2)_4$ to K and Rb: each peroxide ligand bonds two K^+ cations with distances from 2.6–2.9 Å, and one Rb^+ cation with Rb–$O_{peroxide}$ bonds of 3.36 Å. The Nb–$O_{peroxide}$ bond length is 2.00(4) Å, and the O–O peroxide bonds are 1.40(5) Å. For comparison, in the $Rb_3Nb(O_2)_4$ salt, the Nb–$O_{peroxide}$ bond length is 1.991(6) Å, and the O–O peroxide bonds are 1.50(1) Å.[10] Similarly, the $K_3Nb(O_2)_4$ salt has Nb–$O_{peroxide}$ bond lengths from 2.08–2.15 Å, and the O–O distance is 1.35 Å.[11] The two modes of alkali bonding to a peroxide ligand found in **4** are shown in part b of Figure 2: 1) The K^+ is bonded side-on, one bond to each O^- of the peroxide, and 2) the Rb^+ bridges two peroxide ligands. Both of these bonding modes are observed in the salts, $A_3[M(O_2)_4]$; A = K, Rb, Cs, M = Nb, Ta, see Figure 3 (a).

We have also crystallized U_{28} utilizing $Ta(O_2)_4^{3-}$ [Ta-CsK-U_{28} (**5**)] as a templating anion, see experimental. With a formula of $Cs_{15}[(Ta(O_2)_4)Cs_4K_{12}(UO_2(O_2)_{1.5})_{28}]\cdot 11H_2O$ (**5**) is isostructural with **1** and **2**. The structure of the central cations and $Ta(O_2)_4$ anion is not as well-defined as those within the U_{28} capsule of **4**. Nonetheless, the $Nb(O_2)_4$ and $Ta(O_2)_4$ anions provide final R_1 values (%) for **4** and **5** of 3.7 and 7.1 respectively, compared to about 10 for the related phases **2** and **1** with uranyl in the center. This may be ascribed to improved crystal quality and decreased disorder with the strong anion-template. Again, in **5**, the K^+ cations in the pentagonal rings are disordered in two positions. Ten of twelve are best modeled as 2/3rd occupied for K_{outer} and 1/3rd occupied for K_{inner}. The other two pairs are located on special positions (K5-K5a and K3-K3a) and are better modeled as equally-occupied in the outside and inside position. However, not all of the Ta–$O_{peroxide}$ oxygen ligands have been identified, which affects the occupancies of these nearby K^+ cations. We assume the disorder of $Ta(O_2)_4$ in **5** is similar to $Nb(O_2)_4$ in **4**, since the K^+-occupancies are similar. Eight oxygens are found bonded to the central Ta with a Ta–O distance of 1.91–2.01 Å. We set these as 2/3rd occupied, following the model of **4**, and the remaining four oxygen sites that we would expect based on the model of **4** are not readily observable.

Despite the uncertainties in the crystallographic data due to disorder of the central anion, vibrational spectroscopy (infrared) provided clear indication of successful incorporation of $Nb(O_2)_4$ and $Ta(O_2)_4$ into the center of U_{28} in **4** and **5**, respectively. Infrared spectra comparing 1) $K_3Nb(O_2)_4$, $KRbU_{28}$ and Nb-$KRbU_{28}$; and 2) $K_3Nb(O_2)_4$, $KCsU_{28}$ and Ta-$KCsU_{28}$ are shown in Figure 4. The bond vibrations for the uranyl peroxide polyhedra are predominantly observed around 900 cm^{-1}, with a small double-peak at 775 and 800 cm^{-1}. While these are the only peaks (other than lattice water) observed in the IR spectra of $KRbU_{28}$ and $KCsU_{28}$, the spectra of **4** and **5** also have the two major peaks for $Nb(O_2)_4$ and $Ta(O_2)_4$, respectively. The structural data of the central Nb or Ta anion may also be interpreted as mixed oxo and peroxo species; i.e. $MO_4^{3-}/M(O_2)_4^{3-}$. The anion for Nb and Ta is not isolatable as a monomer, therefore we do not have ready spectroscopic characterization for comparison. To this end, we have also synthesized U_{28} utilizing the VO_4^{3-} anion in the synthesis matrix. Continued structural, computational and vibrational (Raman and infrared) studies are ongoing to determine which of the Group V $MO_4^{3-}/M(O_2)_4^{3-}$ anions are preferred in the capsule; and even if this unique chemical environment may be used to capture the unprecedented $(Nb/Ta)O_4^{3-}$.

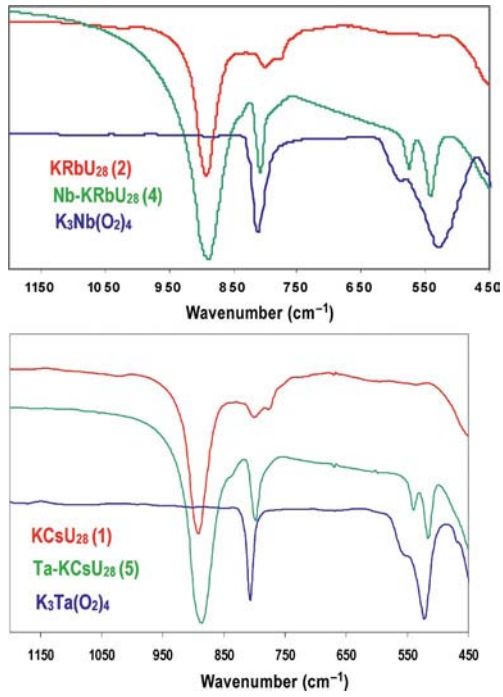

Figure 4. IR spectra showing U_{28} with and without incorporation of the central $M(O_2)_4$ anion [M = Nb for **4**, Ta for **5**].

The color of the uranyl-centered U_{28} salts **1** and **2** are orange-red and the salts of U_{28} with $Nb(O_2)_4$ or $Ta(O_2)_4$ in the center are yellow, see Figure 5. The yellow to red hues of materials containing uranyl species arise from the yl-oxygen to uranium charge-transfer.[12,13] The hue varies as a function of equatorial ligands and U–O_{yl} bond length, and association of the uranyl ligands within its solid-state or solution matrix. Apparently the central uranyl anions of **1** and **2** contribute significantly to the "red-shifted" hues of these crystalline salts, and is the subject of future computational and experimental investigation.

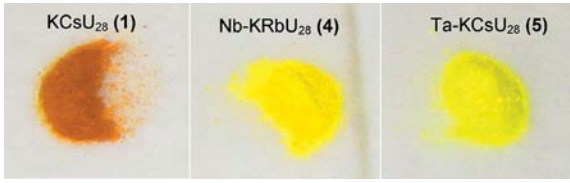

Figure 5. Photographs of $KCsU_{28}$ (**1**), Nb-$KRbCsU_{28}$ (**4**) and Ta-$KCsU_{28}$ (**5**) show the difference in hue between the uranyl-centered clusters and those containing a niobate or tantalate anion at the center.

Cation-templating outside the U_{28} capsule. Compounds **1** and **5**, **2** and **3** exhibit Cs, Rb, and K, respectively, templating on the outside of the U_{28} sphere, and this perhaps influences the solubility and crystallization rate of U_{28}. In both, **1** and **2**, two of the twelve pentagonal rings host a Cs/Rb, bonded to the peroxide ligand oxygens on the outside of the sphere (Figure 6). Likewise in **3**, two pentagonal rings per cluster host a K^+ on the outside convex surface. The U_{28} sphere of **5** also hosts Cs outside two of the twelve pentagonal rings. When both K and Rb, or K and Cs are present in abundance in the crystallization solution, the Rb and Cs are "selected" for bonding the pentagonal ring externally, suggesting these larger alkalis have a templating effect both inside *and* outside the spherical cluster. In **1**, **2**, **3** and **5**, the alkali sited outside the pentagonal ring completes its coordination sphere by bridging to ligand oxygens of a second cluster. The initial crystallization of **1** and **5** from the mother liquor takes place very rapidly, even from relatively dilute solutions. The poorer solubility of these phases is likely directly related to these Cs cations outside and bridging the clusters – Cs salts of other polyoxoanion systems (i.e. polyoxotungstates and polyoxomolybdates) are likewise notoriously insoluble. On the other hand, **4** has no alkalis, neither Rb nor K templating the outside of the pentagonal ring. In this structure, there is a lattice water centered over the outside of each pentagonal ring, but it is not close enough to bond the K^+ inside (K–O distance >4 Å).

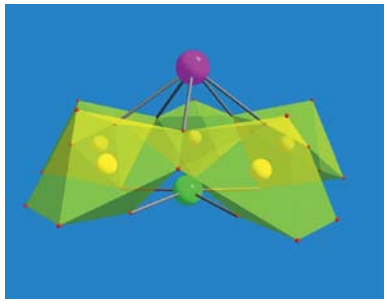

Figure 6. A view of the pentagonal ring in Ta-$KCsU_{28}$ (**5**) showing the inside templating of K^+ (green) and the outside templating of Cs^+ (pink). The five Cs–$O_{peroxide}$ bond lengths shown in this view range from 2.952(7)–3.111(1) Å.

Solution characterization of U_{28}. ^{133}Cs NMR proved ideal to characterize Cs-templated U_{28} in aqueous solution and compare the internal Cs of **1** and **5** that encapsulate the uranyl and the tantalate ions, respectively. While none of the U_{28} analogues described here can be redissolved in pure water, they readily dissolve in TMA^+ (tetramethylammonium), Li^+, Na^+, or K^+ salt or hydroxide solutions. The ^{133}Cs NMR spectra of **1** and **5** are shown in Figure 7. For **5**, the broad peak (+22 ppm, FWHM = 210 Hz) is Cs^+ cations internal to U_{28} and the narrower peak (–1 ppm, FWHM = 15 Hz) is the charge-balancing Cs^+ cations external to U_{28}; and the ratio of the two peaks is about 1:4, matching the formula of the crystalline salt. For **1**, the external Cs peak is much broader, FWHM = 96 Hz. Furthermore, we observe four separate peaks for internal Cs^+ cations, see Figure 7. These are located at 9 (492 Hz), 23 (953 Hz), 36 (521 Hz) and 44 (926 Hz) ppm. The total integration of these internal peaks is approximately 8%, compared to the expected 20% which is observed for **5**, and both the external and internal Cs peaks for **1** are much broader than those of **5**. The multiple internal Cs peaks of **1** compared to the single peak of **5** reinforces the single-crystal X-ray results. There are no monomeric uranyl anions that have tetrahedral symmetry that matches the U_{28} capsule, and therefore this central anion provides more than one type of bonding to the internal Cs, as seen by ^{133}Cs NMR spectroscopy. In contrast, the $Ta(O_2)_4$ anion binds all the internal Cs in an identical manner, giving rise to a single peak. The integration shows that while the Cs in **5** is retained inside the capsule, the Cs in **1** is partially depopulated, likely exiting through the hexagonal windows. Depopulation of the internal Cs of **1** results in higher negative cluster charge, and thus probably some destabilization of the cluster in solution. It is also noteworthy to compare the linewidths of internal and external Cs^+ peaks for **1** and **5** – both are considerably broader for **1**. This is indicative of more exchange between internal and external Cs in **1** compared to **5**. Finally, the external Cs peak of both **1** and **5** are considerably broader than CsCl in identical concentration dissolved in the same TMAOH solution. The peak position and line width of the CsCl is +7.1 ppm with FWHM = 1.2. Thus the shift and broadening [up to ca. 80× in the case of

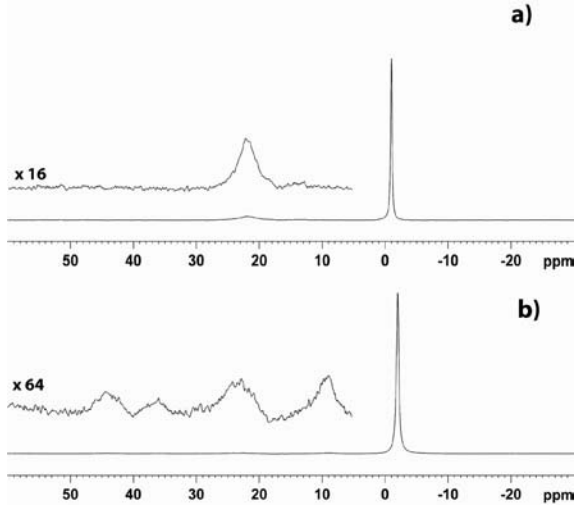

Figure 7. ^{133}Cs NMR spectra of (a) Ta-$KCsU_{28}$ (**5**) and (b) $KCsU_{28}$ (**1**) dissolved in 2 M TMAOH solution, showing the difference in internal templating Cs^+ cations.

1] indicates strong association of the external Cs^+ with the U_{28} anion. In summary, the ^{133}Cs NMR results suggest that the central $Ta(O_2)_4$ anion lends some stability to the U_{28} cluster by providing a more stable bonding environment for the encapsulated Cs, which in turn stabilizes the U_{28} cluster. Moreover, the solution characterization demonstrated here is a clear indication that uranyl peroxide polyanions can indeed be redissolved intact, an important characteristic to facilitate further expansion of this developing field of chemistry.

Dissolution of **5** in 2 M NaOH solution resulted in rapid precipitation of a yellow microcrystalline salt. SEM-EDS (scanning electron microscopy-energy dispersive spectroscopy) revealed the salt had a composition that corresponds exactly with 1) complete exchange of all the internal K^+ for Na^+ 2) retention of the internal Cs^+, and 3) exchange of all external cations for Na^+: i.e. $Na_{15}[(TaO_8)\text{-}Cs_4Na_{12}(UO_2(O_2)_{1.5})_{28}]\cdot xH_2O$ is precipitated [**Na-(5)**]. Figure 8 compares the morphology of **5** and **Na-(5)**. Powder X-ray diffraction and infrared spectroscopy show respectively that this new Na-analogue is a similar lattice as **5**, and the U_{28} cluster remains intact [see Supporting Information for further characterization data for **Na-(5)**]. The IR spectra of **5** and **Na-(5)** are identical, and the powder XRD largely show overlapping peak positions, but with intensity change. This Na salt of U_{28} readily dissolves in water without an added electrolyte! The ^{23}Na NMR of dissolved **Na-(5)** shows a single very broad peak (δ = 3 ppm, FWHM = 360 Hz) suggesting exchange between inner and outer Na^+ occurs. In agreement with the EDS analysis, ^{133}Cs NMR shows only internal Cs^+ peaks: two very broad peaks at +28 and +47 ppm, and no sharp external Cs peak (around 0 ppm). The shift in the internal Cs peak-position indicates the internal U_{28} environment has changed, via the exchange of K for Na. Further characterization of this phase is underway. These spectroscopic characterizations of **Na-(5)** are shown in the Supporting Information. On the other hand, when dissolving **5** in lower concentration of NaOH (i.e. 0.5 M), a new phase crystallizes, which is the subject of ongoing study. Na^+-exchange and cluster rearrangement that were observed in these preliminary experiments requires more investigation, but illustrates an additional pathway to further our understanding of uranyl peroxide cluster chemistry.

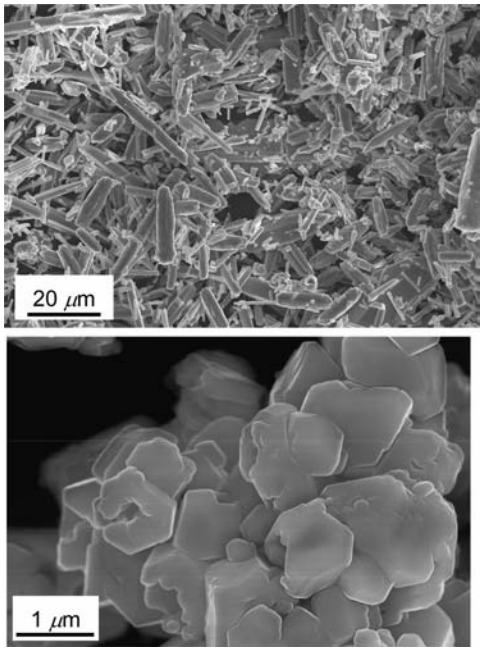

Figure 8. SEM images comparing the morphology of Ta-$KCsU_{28}$ (**5**), top; and **Na-(5)**, bottom, in which all the external Cs and internal K has been exchanged for Na.

Finally, it is noteworthy that radioactive Cs-137 is one of the biggest concerns in alkaline nuclear wastes, in which Na and U are also plentiful. Therefore Cs and/or Na templated and precipitated uranyl clusters is potentially one component of these very complex and dynamic solutions, in that these studies have revealed a strong templating and precipitation effect of Cs for U_{28}, respectively inside and outside the capsule. Furthermore, a recent study[13] has shown that Cs is readily sorbed into studtite, a uranyl peroxide phase that forms on nuclear fuel and in wastes.

Conclusions

As exemplified by U_{28}, cations and anions inside the uranyl peroxide polyanionic clusters play a very important role in assembly of these phases. Furthermore, strategic design of synthesis media that are not dynamic is a key factor in obtaining good yields, pure phases and reproducible procedures. Using these foundational principles, other systems may be explored. For instance, a bowl-like cluster was reported[3f] that has Cs and Na as its countercations. It has Cs sited in the hexagonal rings, but the square rings are empty. This alludes to recent computational studies[5] that suggest Li is the most suitable cation to template the square rings. Perhaps the recently published,[14] water-soluble Cs–Li uranyl-peroxide compound could be utilized to template clusters such as these that feature both square and hexagonal rings. And furthermore, akin to tungstate POMs, open clusters such as these might be templated with oxoanions with stereoactive lone pairs (e.g. $As^{III}O_3$, $Te^{IV}O_2$).[15]

With this suite of U_{28} phases, we can now expand the base of uranyl peroxide cluster chemistry beyond solid-state structures. Studies underway include electrochemistry, solution behavior (ion association, supermolecular assembly, ion-exchange), non-aqueous chemistry, and materials assembly from U_{28} building blocks. Furthermore, this suite of phases with systematic variations provides an ideal opportunity for calorimetry and computational studies to further investigate stabilization effects of the different templating cations and anions. Finally, we are pursuing the development of other suites of uranyl peroxide clusters, building on the knowledge foundation from the study presented here.

Experimental Section

$CsK\text{-}U_{28}$ (1): In a 40 mL beaker, CsCl (0.73 g, 4.3 mmol) is dissolved in 4 mL of 4 molar KOH solution. Three mL 30% H_2O_2

solution is added, and the bubbly warm mixture is cooled in an ice bath to 5 °C. Uranyl nitrate hexahydrate [$UO_2(NO_3)_2$·$6H_2O$; 0.5 g, 1 mmol] is dissolved in 6 mL DI water, also at 5 °C. The uranyl nitrate solution is then added to the CsCl/KOH/H_2O_2 solution while stirring, and continuing to cool in the ice bath. The solution rapidly turns orange and then precipitates a bright yellow solid. This solid is collected quickly by vacuum filtration, and washed with ethanol for rapid drying. A 250 mL beaker is then filled with 100 mL DI water, along with a stirbar. While stirring rapidly, the previously isolated bright yellow powder is added via a spatula to yield a clear orange solution. Soon after stirring is ceased, the solution begins to appear cloudy, upon initial crystallization of KCs-U_{28}. This solution is covered and set in a refrigerator (8 °C) for several days until it no longer appears cloudy. The crystalline orange-yellow precipitate is collected by vacuum filtration and washed with ethanol; yield 0.26 g, 57% based on uranium.

RbK-U_{28} (2): The first step of this synthesis is identical to that of **1**, except RbCl (0.50 g, 4.1 mmol) is substituted for CsCl. A 50 mL beaker is then filled with 30 mL DI water, along with a stirbar. While stirring rapidly, the previously-isolated bright yellow precursor powder is added via a spatula to yield a clear orange solution. This beaker is then set in the fumehood to initialize crystallization via evaporation. After about 24 h, cloudiness and crystal growth is observed, and the beaker is placed in a refrigerator for up to 10 d. Large amber ca. 0.2×0.05 mm acicular crystals are collected by vacuum filtration and washed with ethanol; yield 0.26 g, 61% based on uranium.

Nb-RbK-U_{28} (4): The first step proceeds the same as that of **1** and **2**, but neither Rb nor Cs was included in the synthesis of this precursor salt. $Rb_8[Nb_6O_{19}]$·$16H_2O$ (synthesis described prior[8b]) (0.1 g, 0.33 mmol Nb) was dissolved in 30 mL DI water, and the potassium uranyl peroxide precursor salt was added while stirring at room temperature. The beaker was left in the fume hood for evaporation for six days to yield a crop of dodecahedral yellow crystals; yield 0.22 g, ca. 52% based on uranium.

Ta-CsK-U_{28} (5): The same procedure is followed for the synthesis of **1**, but $K_3Ta(O_2)_4$ (synthesis described prior[8a]) (0.1 g, 0.2 millimol) is initially dissolved in the 100 mL of DI water, before adding the KCs-UO_2 yellow precursor for the U_{28} compounds. Again, clouding of the orange liquid is observed almost immediately. The precipitating solution is set in the refrigerator for three days to continue crystallization. The bright yellow microcrystalline product is collected by vacuum filtration and washed with ethanol; yield 0.33 g, 74% yield, based on uranium.

Characterization Techniques

Single-Crystal X-ray Diffraction: Single-crystal X-ray diffraction of **1**, **2**, **4** and **5** were performed at 100 K on a Bruker AXS SMART-CCD diffractometer with graphite monochromated Mo-K_α (0.71073 A) radiation. Data collection and reduction were carried out with SMART 5.054 (Bruker, 1998) and SAINT 6.02 (Bruker, 2001) software, respectively. Empirical absorption correction was applied using SADABS. The structures were solved by Direct Methods (program SIR97) and refined by full-matrix least-squares on F^2 (SHELX97). All subsequent structure solution and refinement were performed within the WinGX system. Pertinent crystallographic information is summarized in Table 2.

Further details on the crystal structure investigations may be obtained from the Fachinformationszentrum Karlsruhe, 76344 Eggenstein-Leopoldshafen, Germany (Fax: +49-7247-808-666; E-mail: crysdata@fiz-karlsruhe.de), on quoting the depository number CSD-422382 (for **1**), -422383 (for **2**), -422380 (for **4**), and -422381 (for **5**).

^{133}Cs and ^{23}Na NMR Spectroscopy: NMR spectra were obtained on a Bruker Avance III 600 at 78.72 MHz for ^{133}Cs and 158.75 MHz for ^{23}Na using a 5 mm broadband probe. The ^{133}Cs and ^{23}Na chemical shifts were eferenced to the secondary external sample of 1 M CsCl (δ = 0 ppm) and 1 M NaCl (δ = 0 ppm), respectively.

Infrared Spectroscopy: Fourier transform infrared (FTIR) spectra for of **1**, **2**, **3**, **4** and **5** were collected on a PerkinElmer Spectrum One instrument. Powders of uranyl salts were mixed into KBr matrix and pressed into pellets for analysis. The IR spectra of the $M(O_2)_4^{3-}$ (M = Nb, Ta) salts were collected on a Thermo Nicolet 380 FT-IR instrument equipped with a SMART Orbit ATR accessory.

SEM-EDS: Scanning electron microscopy-Energy dispersive spectroscopy was used to analyze composition of U_{28} phases, particularly to confirm ratios of K:Cs and K:Rb. In every case, the analyses agreed well with the identification via the single-crystal X-ray data.

Powder X-ray Diffraction: Spectra of bulk powders of **1**, **2**, **4** and **5** were measured on a Bruker D8-Advance; specimens were prepared as smear-mounts at rotated at 20 rpm during data collection.

Thermogravimetry was utilized to confirm the amount of lattice water.

Supporting Information (see footnote on the first page of this article): Four figures showing additional characterization data of U_{28} salts.

Acknowledgments

This material is based upon work supported as part of the Materials Science of Actinides, an Energy Frontier Research Center funded by the U. S. Department of Energy, Office of Science, Office of Basic Energy Sciences under award number DE-SC0001089. We thank Gary L. Zender (SNL) for the scanning electron micrographs. Sandia is a multiprogram laboratory operated by Sandia Corporation, a Lockheed-Martin Company for the U. S. Department of Energy under contract number DE-AC04-94AL85000.

[1] a) A. Rey, S. Utsusunomiya, J. Giménez, I. Casas, J. dePablo, R. C. Ewing, *Am. Mineral. Am. Mineral. Am. Mineral. Am. Mineralogist* **2009**, *94*, 229–235; b) B. McNamara, E. C. Buck, B. Hanson, *Materials Research Society Symposium Proceedings, Scientific Basis for Nuclear Waste Management XXVI* **2003**, *757*, p. 401–406; c) B. Hanson, B. McNamara, E. C. Buck, J. Friese, E. Jenson, K. Krupka, B. Arey, *Radiochim. Acta* **2005**, *93*, 159–168; d) K. A. Hughes, P. C. Burns, *Am. Mineral.* **2003**, *88*, 1165–1168; e) K. A. Hughes-Kubatko, K. B. Helean, A. Navrostky, P. C. Burns, *Science* **2003**, *302*, 1191–1193; f) C. Corbel, G. Sattonnay, S. Guilbert, F. Garrido, M. F. Barthe, C. Jegou, *J. Nucl. Mater.* **2006**, *348*, 1–17; g) G. Sattonnay, C. Ardois, C. Corbel, J. F. Lucchini, M. F. Barthe, F. Garrido, D. Gosset, *J. Nucl. Mater.* **2001**, *288*, 11–19.

[2] a) M. Douglas, S. B. Clark, J. I. Friese, B. W. Arey, B. D. Hanson, *Environ. Sci. Technol.* **2005**, *39*, 4117–4124; b) P. C. Burns, R. C. Ewing, M. L. Miller, *J. Nucl. Mater.* **1997**, *245*, 1–9; c) E. C. Buck, R. J. Finch, P. A. Finn, J. K. Bates, *Eur. Mater. Res. Soc. Symp. Proc.* **1998**, *506*, 83–91; d) P. C. Burns, K. M. Deely, S. Skanthakumar, *Radiochim. Acta* **2004**, 151–159; e) P. C. Burns, K. A. Kubatko, G. Sigmon, B. J. Fryer, J. E. Gagnon, M. R. Antonio, L. Soderholm, *Angew. Chem. Int. Ed.* **2005**, *44*, 2135–2139.

[3] a) T. Z. Forbes, J. G. McAlpin, R. Murphy, P. C. Burns, *Angew. Chem. Int. Ed.* **2008**, *47*, 2824–2827; b) G. E. Sigmon, J. Ling,

D. K. Unruh, L. Moore-Shay, M. Ward, B. Weaver, P. C. Burns, *J. Am. Chem. Soc.* **2009**, *131*, 16648–16649; c) G. E. Sigmon, D. K. Unruh, J. Ling, B. Weaver, M. Ward, L. Pressprich, A. Simonetti, P. C. Burns, *Angew. Chem. Int. Ed.* **2009**, *48*, 2737–2740; d) D. K. Unruh, A. Burtner, P. C. Burns, *Inorg. Chem.* **2009**, *48*, 2346–2348; e) D. K. Unruh, A. Burtner, L. Pressprich, G. E. Sigmon, P. C. Burns, *Dalton Trans.* **2010**, *39*, 5807–5813; f) G. E. Sigmon, B. Weaver, K. A. Kubatko, P. C. Burns, *Inorg. Chem.* **2009**, *48*, 10907–10909; g) J. Ling, J. Qiu, G. E. Sigmon, M. Ward, J. E. S. Szymanowski, P. C. Burns, *J. Am. Chem. Soc.* **2010**, *132*, 13395–13402; h) J. Ling, C. M. Wallace, J. E. S. Szymanowski, P. C. Burns, *Angew. Chem. Int. Ed.* **2010**, *49*, 7271–7273.

[4] N. E. Brese, M. O'Keefe, *Acta Crystallogr., Sect. B* **1991**, *47*, 192–197.

[5] P. Miro, S. Pierrefixe, M. Gicquel, A. Gil, C. Bo, *J. Am. Chem. Soc.* **2010**, *132*, 17787–17794.

[6] In each of these U_{28} structures, at least one internal alkali is bonded to a water that sits directly outside the cluster, centered over the hexagonal ring.

[7] The orthorhombic *Cmcm* "doubled" cell akin to that of **3** was also considered for **1**, **2** and **5**, but it did not yield good solutions.

[8] a) T. M. Anderson, M. A. Rodriguez, F. Bonhomme, J. Bixler, T. M. Alam, M. Nyman, *Dalton Trans.* **2007**, 4517–4522; b) M. Nyman, T. M. Alam, F. Bonhomme, M. A. Rodriguez, C. S. Frazer, M. E. Welk, *J. Cluster Sci.* **2006**, *17*, 197–219.

[9] D. Bayot, M. Devillers, *Coord. Chem. Rev.* **2006**, *250*, 2610–2626.

[10] H. Haeuseler, M. Wagener, H. Mueller, *Z. Naturforsch. Teil B* **1997**, *52*, 1082–1086.

[11] I. A. Wilson, *Ark. Kemi Mineral. Geol.* **1942**, *15*, 1–7.

[12] R. G. Denning, *J. Phys. Chem. A* **2007**, *111*, 4125–4143.

[13] J. Gimenez, X. Martinez-Llado, M. Rovira, J. dePablo, I. Casas, R. Sureda, A. Martinez-Esparza, *Radiochim. Acta* **2010**, *98*, 4793.

[14] M. Nyman, M. A. Rodriguez, C. F. Campana, *Inorg. Chem.* **2010**, *49*, 7748–7755.

[15] C. Ritchie, K. G. Alley, C. Boskovic, *Dalton Trans.* **2010**, *39*, 8872–8874.

Received: December 27, 2010
Published Online: March 4, 2011

